Postharvest Biology and Technology 67 (2012) 130–137

Contents lists available at SciVerse ScienceDirect

Postharvest Biology and Technology

journal homepage: www.elsevier.com/locate/postharvbio

Ultrasonic evaluation of the hydration degree of the orange peel

N. Jiménez, R. Picó, F. Camarena*, J. Redondo, B. Roig

Institut d'Investigació per a la Gestió Integrada de les Zones Costaneres, Universitat Politècnica de València, C/Paranimf 1, 46730 Grao de Gandia, Spain

ARTICLE INFO

Article history:
Received 28 March 2011
Accepted 31 December 2011

Keywords:
Ultrasound
Postharvest quality
Orange peel
Hydration degree
Young modulus
Rayleigh wave
Elastodynamic
Finite-Differences Time-Domain, FDTD

ABSTRACT

The elastic parameters of fruit and vegetables are normally monitored in quality control processes as there is a good correlation to the degrees of firmness, turgidity and humidity. These parameters have been traditionally measured by means of penetration tests, which are destructive. This has resulted in the increased attention recently given to ultrasonic techniques applied to the quality evaluation of horticultural commodities. Nevertheless, since most of the fruit and vegetables display a viscoelastic behavior, the penetration test should be considered to be quasi-static, especially when compared with the speeds associated with the ultrasonic tests. Both methods should provide different values for the elastic parameters. The aim of this work is to study this discrepancy in the values of the elastic parameters and interpret the elastodynamic behavior of the vegetable tissue under an ultrasound test. Thus, the paper presents an ultrasonic nondestructive method to evaluate the elastic parameters of the sweet orange peel at 40 kHz. The complete dehydration process of two sets of oranges (Navelina and Ortanique) was monitored for 2 months. A linear elastic solid model with viscous losses was numerically solved using a simulation scheme based on a 3D-Spherical FDTD method (Finite-Difference Time-Domain) in order to interpret the results, which proved that the elastic parameters obtained by penetration and ultrasonic tests differ. The method provides an empirical relation between the hydration state and the elastic parameters of the orange peel. Therefore, the proposed ultrasonic test reported in this work is capable of determining the hydration state of the orange simply by measuring the propagation speed of the Rayleigh waves on the orange peel, and hence, can be used as a fruit quality index during postharvest processes.

© 2012 Elsevier B.V. All rights reserved.

1. Introduction

In the context of modern agriculture and its competitive markets there is growing interest regarding the need to evaluate the quality of fruit and vegetables. Quality is a subjective term consisting of many properties or characteristics such as sensory properties (appearance, texture, taste or smell) that have to be examined by people, and mechanical and functional properties, in addition to nutritive values, chemical constituents, and the absence of defects. Mindful of this, instrumentation and methods to measure quality-related attributes have been developed over the last 80 years, most recently in an attempt to establish non-destructive and real-time systems. In order to evaluate texture attributes, the mechanical properties are usually measured (Abbot, 1999). The traditional methods for evaluating these properties (such as Young's Modulus, and also the rupture force and bioyield force) are puncture or compression tests made at relatively low probe speeds ($\ll$1 m/s), typical of such instruments as the Magness–Taylor fruit firmness tester and the electronic universal (Force/Deformation) testing instruments, which are quasi-static. Acoustic methods are also used for quality evaluation (accounting for approximately 20% of the nondestructive techniques, Butz et al., 2005). In specifically, ultrasonic devices and measuring techniques have been developed over the last two decades to evaluate the mechanical properties of tissue, allowing the nondestructive monitoring of some physiochemical, biochemical and mechanical changes that occur in fruit tissues during the various stages of their pre- and postharvest existence. Some examples of these can be found in Mizrach (2000), Flitsanov et al. (2000), Verlinden et al. (2004), Bechar et al. (2005) and Gaete-Garreton et al. (2005). A review of the different ultrasonic techniques used for determining the material properties of fresh fruit and vegetable tissues during the last two decades can be found in Mizrach, 2008. Some of these techniques have been used in the past to find correlations between ultrasonic velocity and absorption through the orange peel and turgidity and the hydration state of oranges (Camarena and Martinez-Mora, 2006; Camarena et al., 2007). These techniques can also be used to evaluate the elastic parameters of the orange peel and consequently the hydration degree, as it will be demonstrated in this work.

The information of changes in postharvest physico-mechanical properties (elastic parameters) of the orange peel and the fruit under ambient and refrigerated storage conditions is important to help to determine the appropriate handling, packaging, storage and transportation systems (Singh and Sreenivasula, 2006).

* Corresponding author. Tel.: +34 96 284 93 00; fax: +34 96 284 93 09.
E-mail address: fracafe@fis.upv.es (F. Camarena).

0925-5214/$ – see front matter © 2012 Elsevier B.V. All rights reserved.
doi:10.1016/j.postharvbio.2011.12.020

Table 1
Quasi-static measured elastic properties, calculated longitudinal (c_{bulk}) and shear (c_{shear}) wave speed, and ultrasonic measured speed of various fruits and vegetables.

Fruits	Quasi-static measured parameters			Calculated speed		Measured speed (Krautkramer and Krautkramer, 1990)
	Density ρ (kg/m^3)	Young Modulus E (MPa)	Poisson's ratio ν	c_{bulk} (m/s)	c_{shear} (m/s)	c (m/s)
Orange (Singh and Sreenivasula, 2006)	903	1.57	0.34	82.7	54.6	130–240
Avocado (Baryeh, 2000)	963	0.48	0.33	32.1	18.2	150–400
Apple (Grotte et al., 2002)	1003	3.33	0.17	65.1	36.5	98–183
Potato (Jindal and Techasena, 1985)	1087	7.14	0.25	60.8	34.1	686.9
Carrot (Bunyaphlanan, 1973)	1021	6.96	0.30	104.1	64.1	341–500

List of symbols used.

Symbol	Magnitude	Symbol	Magnitude
$\boldsymbol{\tau}$	Stress tensor	$\boldsymbol{\nu}$	Particle velocity vector
λ	Lame's 1st parameter	μ	Lame's 2nd parameter
E	Young modulus	ν	Poisson's ratio
Dh	Dehydration	ρ	Bulk density
f	Frequency	r	Radial coordinate
θ	Azimuth angle coordinate	φ	Elevation angle coordinate
c	Propagation speed (measured)	c_P	Pressure wave propagation speed
c_R	Rayleigh wave propagation speed	c_S	Shear wave propagation speed
η_P	Resistance coefficient longitudinal wave	η_S	Resistance coefficient shear wave
N_λ	Discrete elements per wavelength	λ_L	Longitudinal wavelength
Δt	Numerical time step	Δr	Radial element length
$\Delta\theta$	Azimuth angle element length	$\Delta\varphi$	Elevation angle element length
α_{max}	PML scaling factor	Ω_{max}	PML attenuation factor

The orange, just as most of the other juicy fruits such as the tomato, cherry and various berry fruits, exhibits viscoelastic behavior. This signifies that the elastic parameters depend not only on the force and deformation, but also on the time factor (Abbot, 1999). Regarding this, the elastic parameters obtained with quasi-static techniques may differ from those obtained using ultrasonic techniques. Evidence can be seen in Table 1 that displays a review of the elastic parameters measured by means of quasi-static procedures for different fruits, the bulk and shear speed calculated from these parameters and the speed evaluated from ultrasonic experiments. These experiments can be destructive, if inner parts of the fruit are directly measured, or non destructive, if the ultrasonic wave is excited and detected in the surface of the fruit. However, the speed measurements are always associated to shear or surface waves, as it will be demonstrated in this work. There is a clear disagreement between the calculated and measured speeds for all the fruits, and it is one of the objectives of this work to clarify this disagreement.

In this work an ultrasonic nondestructive method is proposed to evaluate the elastic parameters of the orange fruit. Two sets of oranges, Navelina and Ortanique, have been monitored ultrasonically during the entire dehydration process (2 months). From an elastodynamic point of view, the entire orange has been discomposed into three spherical shells corresponding anatomically to the flavedo (fruit peel), albedo and inner carpels tissue of the orange fruit. A linear elastic model has been proposed and a computational method based on FDTD (Finite-Differences Time-Domain) scheme has been implemented in order to simulate the propagation of the ultrasonic waves through these three layers. It has allowed us to clarify the nature of the different waves traveling through the orange, to demonstrate that the waves measured by our device are surface waves and also that the quasi-static parameters are incoherent with the ultrasonic framework.

2. Experimental set-up and measurement procedure

An experimental transmitter-receiver device was designed to excite and detect acoustic waves on the surface of the orange as can be observed in Fig. 1. A harmonic wave function generator (Agilent model 33220A, Agilent Technologies Canada, Mississauga, ON, USA) and a power amplifier (ENI model 240L, ENI, Rochester, NY, USA) were used to excite a 40 kHz ultrasonic sandwich transducer built in our laboratory. An identical transducer was used for reception, and an oscilloscope for data acquisition and analysis. Two aluminum ultrasonic energy concentrators were used to match the surface diameters of the transducers, i.e., 14 mm, to the desired area of contact with the fruit, a diameter of 2.1 mm, using conical reduction and a flat tip shape.

The transducers were mounted on a goniometer in order to change the angle between their axis, thereby changing the gap between the transducer tips (between 2 and 10 mm) and permitting a perpendicular contact between the concentrators and the orange peel. A system of springs at the bottom of the transducers controlled the contact force applied to the fruit peel, which was maintained constant at 2 N. This particular force was chosen in trial and error tests as compromised between sufficient contacts force and preventing of tip penetration into the fruit tissue.

Emitted waves penetrated the peel and propagated through the adjacent tissue along the gap between the probe tips. Wave speed was calculated by measuring the time of flight at different gaps (2, 4, 6 and 8 mm) and fitting a line. The attenuation coefficient was calculated by looking at the exponential decay of the received wave amplitude at the same gap distances (Krautkramer and Krautkramer, 1990).

On 30 January 2010, two batches of oranges were harvested from the same field (La Safor, Valencia, Spain): a set of seven Navelina sweet oranges (*Citrus sinensis*, L. Osbeck) with a similar size (mean diameter 7.1 cm and S.D. 0.3 cm), weight (mean weight 191 g and S.D. 26 g) and maturity, and a set of seven Ortanique oranges, a hybrid of the tangerine and sweet orange (*Citrus sinensis* × *Citrus reticulata*) also of a similar size (mean diameter 6.7 cm and S.D. 0.2 cm), weight (mean weight 130 g and S.D. 13 g) and maturity. No specific chemical processing was applied to the fruit and it was stored under ambient conditions (20–23 °C and 49–53% relative humidity).

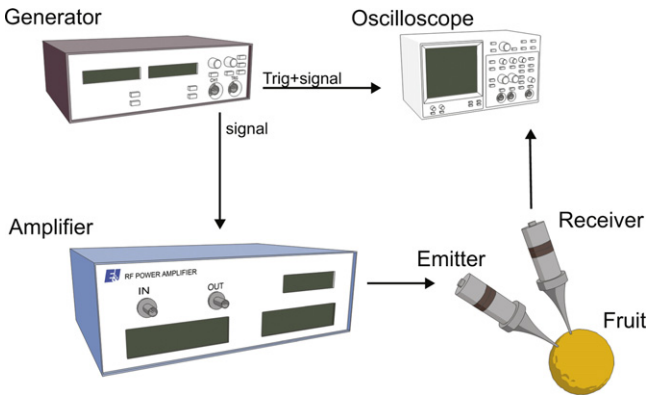


Fig. 1. Diagram of the ultrasonic measuring system.

Table 2
Mechanical parameters used in the simulations for the two models.

Parameter	Air	Flavedo	Albedo	Inner core
Density, ρ (kg/m^3)	1.21	903	820	978
Lame's 1°, λ (MPa)	0.142	1.95×10^3	0.62×10^3	2.2×10^3
Lame's 2°, μ (MPa)	0	36	10.8	0
Young modulus, E (MPa)	–	107.3	22.2	–
Poisson's ratio, ν	–	0.491	0.25	–

The seven Navelina and the seven Ortanique oranges were monitored for their ultrasonic properties and degree of dehydration over 65 d. The extent of dehydration was evaluated from the weight loss, as explained in Camarena and Martinez-Mora (2006) and Camarena et al. (2007).

3. Numerical simulation

With the aim of understanding the nature of the wave detected by the ultrasonic experimental device, a FDTD simulation has been implemented. An inverse method to obtain the elastic parameters from the speed measurements has been used. Thus, the wave propagation speed has been experimentally measured in the fruit surface and a compressional sound speed similar than water has been assumed. From these sound speed values the elastic properties of the orange peel has been calculated and finally simulation was launched with these parameters to check that the received waves in that simulation are the same that the measured ones. The concordance was checked by study the polarization of the waves and the sound speed in the media detected by the simulated ultrasonic device. This procedure has been widely used in other fields such as geophysics, where it is used to obtain the mechanical characteristics of the soil (Banab and Motazedian, 2010) and in biomechanics where it helps to characterize biological tissue such as bones (Bossy et al., 2004).

The proposed simulation considers a physical model for the orange (a linear elastic solid) and a set of boundary conditions (three spherical layers with different levels of thickness according to the characteristics of the orange), and also presupposes the values of the elastic parameters of each of these layers (as shown in Table 2). From an elastodynamic perspective, the orange tissue can be divided into three different layers. Firstly, the outermost part of the fruit peel is the orange pigmented shell known as the flavedo, where, embedded in the pits, are the many volatile oil glands. On the reverse side of the flavedo, there is a porous white layer, the albedo. Finally, the water-like tissue core of the orange is composed of fluid-filled vesicles called carpels which contain the orange juice and seeds (Agusti, 2000).

Due to the elevated water content in fruit's peel (about 75% of the peel mass is water, 296% dry basis (Singh and Sreenivasula, 2006)) it is reasonable to believe that a linear acoustic fluid model for wave propagation would be appropriate to study the elastic parameters of the orange peel. This model is able to predict the directivity pattern of the sound pressure field (Mizrach et al., 2009). However, as will be observed from our study, longitudinal acoustic waves are incapable of explaining the low values obtained for the wave velocity in the experiments. Transverse wave propagation should be taken into account. As such, it is necessary to incorporate the shear elasticity within the model. In order to do so, the well-established model for a linear elastic solid is proposed; that is a solid for which the strain is fully determined by the stress. Additionally, as the cell structure of the orange is very small in comparison with the typical wavelength of ultrasound on these media (5 mm for shear waves and 3.8 cm for longitudinal waves at 40 kHz), it can be assumed that the tissue is homogeneous and can be fully described by its linear elastic properties.

The main equations of the model can be deduced from Newton's second law and Hooke's law (Auld, 1973). In velocity-stress lossless formulation this can be written as:

$$\frac{\partial \boldsymbol{\tau}}{\partial t} = \lambda \bar{\mathbf{I}}(\Delta \cdot \boldsymbol{\nu}) + \mu(\nabla \boldsymbol{\nu} + \boldsymbol{\nu}\nabla) \tag{1}$$

$$\rho \frac{\partial \boldsymbol{\nu}}{\partial t} = \nabla \cdot \boldsymbol{\tau} \tag{2}$$

where $\boldsymbol{\tau}$ is the stress tensor, and $\boldsymbol{\nu}$ is the particle displacement velocity vector. This model accounts for the propagation of volumetric waves (longitudinal and transverse) as well as surface acoustic waves (Rayleigh, 1885).

Due to the spherical shape of the orange, the most straightforward way to solve the problem is to express Eqs. (1)–(2) in the spherical coordinate system (r, θ, φ), where r is the radial distance, θ is the azimuth and φ the elevation angle. For the ith component $i = (r, \theta, \varphi)$ the particle velocity v_i is:

$$\begin{aligned}
\rho \frac{\partial v_r}{\partial t} &= \frac{\partial \tau_{rr}}{\partial r} + \frac{1}{r}\frac{\partial \tau_{r\theta}}{\partial \theta} + \frac{1}{r\,sin\theta}\frac{\partial \tau_{r\phi}}{\partial \phi} + \frac{2\tau_{rr} - \tau_{\theta\theta} - \tau_{\phi\phi} + \tau_{r\theta}\cot\theta}{r} \\
\rho \frac{\partial v_\theta}{\partial t} &= \frac{1}{r}\frac{\partial \tau_{\theta\theta}}{\partial \theta} + \frac{\partial \tau_{r\theta}}{\partial r} + \frac{1}{r\,sin\theta}\frac{\partial \tau_{\theta\phi}}{\partial \phi} + \frac{3\tau_{r\theta} + (\tau_{\theta\theta} - \tau_{\phi\phi})\cot\theta}{r} \\
\rho \frac{\partial v_\phi}{\partial t} &= \frac{1}{r\,\sin\theta}\frac{\partial \tau_{\phi\phi}}{\partial \phi} + \frac{\partial \tau_{r\phi}}{\partial r} + \frac{1}{r}\frac{\partial \tau_{\theta\phi}}{\partial \theta} + \frac{3\tau_{r\phi} + 2\tau_{\theta\phi}\cot\theta}{r}
\end{aligned} \tag{3}$$

And for the normal stress τ_{ii}:

$$\begin{aligned}
\frac{\partial \tau_{rr}}{\partial t} + \eta_p \tau_{rr} &= \lambda\left(\frac{\partial v_r}{\partial r} + \frac{2}{r}v_r + \frac{1}{r}\frac{\partial v_\theta}{\partial \theta} + \frac{\cot\theta}{r}v_\theta + \frac{1}{rsin\theta}\frac{\partial v_\phi}{\partial \phi}\right) + 2\mu\frac{\partial v_r}{\partial r} \\
\frac{\partial \tau_{\theta\theta}}{\partial t} + \eta_p \tau_{\theta\theta} &= \lambda\left(\frac{\partial v_r}{\partial r} + \frac{2}{r}v_r + \frac{1}{r}\frac{\partial v_\theta}{\partial \theta} + \frac{\cot\theta}{r}v_\theta + \frac{1}{rsin\theta}\frac{\partial v_\phi}{\partial \phi}\right) + 2\mu\left(\frac{v_r}{r} + \frac{1}{r}\frac{\partial v_\theta}{\partial \theta}\right) \\
\frac{\partial \tau_{\phi\phi}}{\partial t} + \eta_p \tau_{\phi\phi} &= \lambda\left(\frac{\partial v_r}{\partial r} + \frac{2}{r}v_r + \frac{1}{r}\frac{\partial v_\theta}{\partial \theta} + \frac{\cot\theta}{r}v_\theta + \frac{1}{rsin\theta}\frac{\partial v_\phi}{\partial \phi}\right) + 2\mu\left(\frac{v_r}{r} + \frac{\cot\theta}{r}v_\theta + \frac{1}{rsin\theta}\frac{\partial v_\phi}{\partial \phi}\right)
\end{aligned} \tag{4}$$

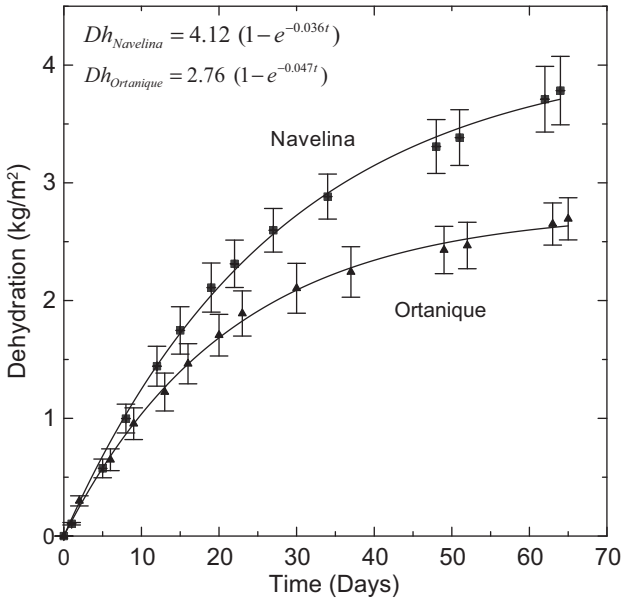


Fig. 2. Dehydration of oranges during storage under ambient conditions. Uncertainty bars show the standard deviation of the values obtained for 7 oranges.

Finally for the $i=(r,\theta,\varphi)$, $j=(r,\theta,\varphi)$ and $i \neq j$ the shear stress τ_{ij} components can be expressed as:

$$\begin{aligned}
\frac{\partial \tau_{r\theta}}{\partial t} + \eta_s \tau_{r\theta} &= \mu \left(\frac{1}{r}\frac{\partial v_r}{\partial \theta} - \frac{v_\theta}{r} + \frac{\partial v_\theta}{\partial r} \right) \\
\frac{\partial \tau_{r\phi}}{\partial t} + \eta_s \tau_{r\phi} &= \mu \left(\frac{1}{r \sin\theta}\frac{\partial v_r}{\partial \phi} - \frac{v_\phi}{r} + \frac{\partial v_\phi}{\partial r} \right) \\
\frac{\partial \tau\theta\phi}{\partial t} + \eta_s \tau_{\theta\phi} &= \mu \left(\frac{1}{r \sin\theta}\frac{\partial v_\theta}{\partial \phi} + \frac{1}{r}\frac{\partial v_\phi}{\partial \theta} - \frac{\cot\theta}{r}\partial_\phi \right)
\end{aligned} \quad (5)$$

η_P, η_S are the resistance coefficients related to the attenuation coefficient of the longitudinal and shear waves respectively (Hosokawa, 2008). The singularity at $r=0$ and $\theta=0$ is taken into account in the definition of the numerical scheme by excluding the center of the sphere and the plane $\theta=0$ from the computational domain.

An explicit Finite-Difference Time-Domain method (FDTD) was used to simulate the elastodynamic behavior of the orange fruit. Thus, the linear solid equations are discretized using second order central difference approximations for the space and time partial derivatives and solved by a *leap-frog* scheme (Schröder and Scott, 2002; Chen and Chew, 1998; Chew and Liu, 1996). This leads to a spatially staggered discretization of the velocity, the normal and shear stress fields, and a temporal staggered discretization of the particle velocity vector and stress tensor.

The numerical model for the orange is defined by a domain divided into three concentric spherical shells. The surrounding outer layer of the orange domain is air. The first layer is the fruit's external orange shell, the flavedo (2 mm thick with a 50 mm curvature radius), next is the inner layer, the albedo (3 mm thick with a 48 mm curvature radius) and finally, the inner core (45 mm of curvature radius). The mechanical features of the materials selected for the simulation are listed in Table 2 and their use is justified in Section 5 of this paper.

The unit cell of the spherical mesh consists of a pyramidal frustum element of appropriate length to limit the numerical dispersion of the computational method. To ensure this, the number of elements per wavelength (N_λ) must be higher than 10 for all elastic waves. Therefore, the length of the unit cell is chosen according to

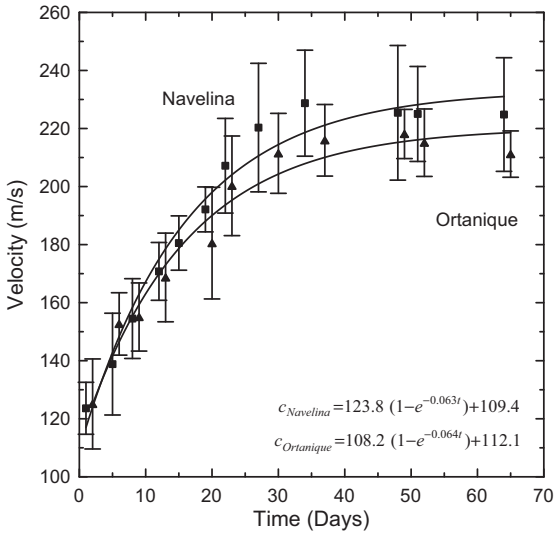


Fig. 3. Ultrasonic wave speed in the orange during storage under ambient conditions. Uncertainty bars show the standard deviation of the values obtained for 10 oranges.

Table 3
Parameters obtained from the fit of experimental data to the theoretical expressions for dehydration and velocity.

Variety	Dehydration			Velocity			
	a (kg/m²)	b	R^2	c_0 (m/s)	a (m/s)	b	R^2
Navelina	4.12	0.036	0.99	109.4	123.8	0.063	0.97
Ortanique	2.76	0.047	0.99	112.1	108.2	0.064	0.97

Eq. (6): the dispersion is determined by the minimal elastic wave speed and the maximum frequency of the signal in all subdomains:

$$N_\lambda = \frac{c_{\min}\sqrt{(\Delta r)^{-2} + (r_{\max}\Delta\theta \sin\Delta\phi)^{-2} + (r_{\max}\Delta\phi)^{-2}}}{f_{\max}} \geq 10 \quad (6)$$

Thus, the highest element's diagonal is 3.025×10^{-5} m, which leads to 10.8 and 142.1 elements per wavelength for transversal waves and for longitudinal waves respectively at a frequency of 40 kHz in the peel layer. The temporal step (Δt) of the algorithm was selected to preserve a maximum Courant number of 0.9 over all subdomains, and to ensure that the stability conditions at media interface are satisfied (Hosokawa, 2008). According to the rectangular coordinates, the CFL stability condition for the spherical FDTD scheme is governed by the highest elastic wave speed (c_{max}) and the smallest element's diagonal over all subdomains:

$$\Delta t \leq \frac{1}{c_{\max}\sqrt{(\Delta r)^{-2} + (r_{\min}\Delta\theta \sin\Delta\phi)^{-2} + (r_{\min}\Delta\phi)^{-2}}} \quad (7)$$

Note that these relations (6) and (7) are empirical expression based on our numerical experiments, like the stability conditions in (Chen and Chew, 1998) for cylindrical coordinates. In order to reduce the computational cost of the numerical scheme, only a sector of the total orange domain has been simulated, and a Perfect Matched Layer (PML) was used to absorb reflections at the boundaries. The PML implementation was based on the time-dependent form of the complex coordinate stretching formulation (Chew and Liu, 1996), with a quadratic profile and the PML scaling and attenuation coefficients values of $\alpha_{max} = N_\lambda/2$ and $\Omega_{max} = \alpha_{max}\, 2\pi f_{max}$ rad/s respectively. Thus, a PML layer was designed with a width of 20 elements, $\Omega_{max} = 2.56 \times 10^6$ rad/s and $\alpha_{max} = 5.4$. The excitation signal was a negative normalized second derivative of a Gaussian function, also known as a Ricker wavelet, centered at 40 kHz.

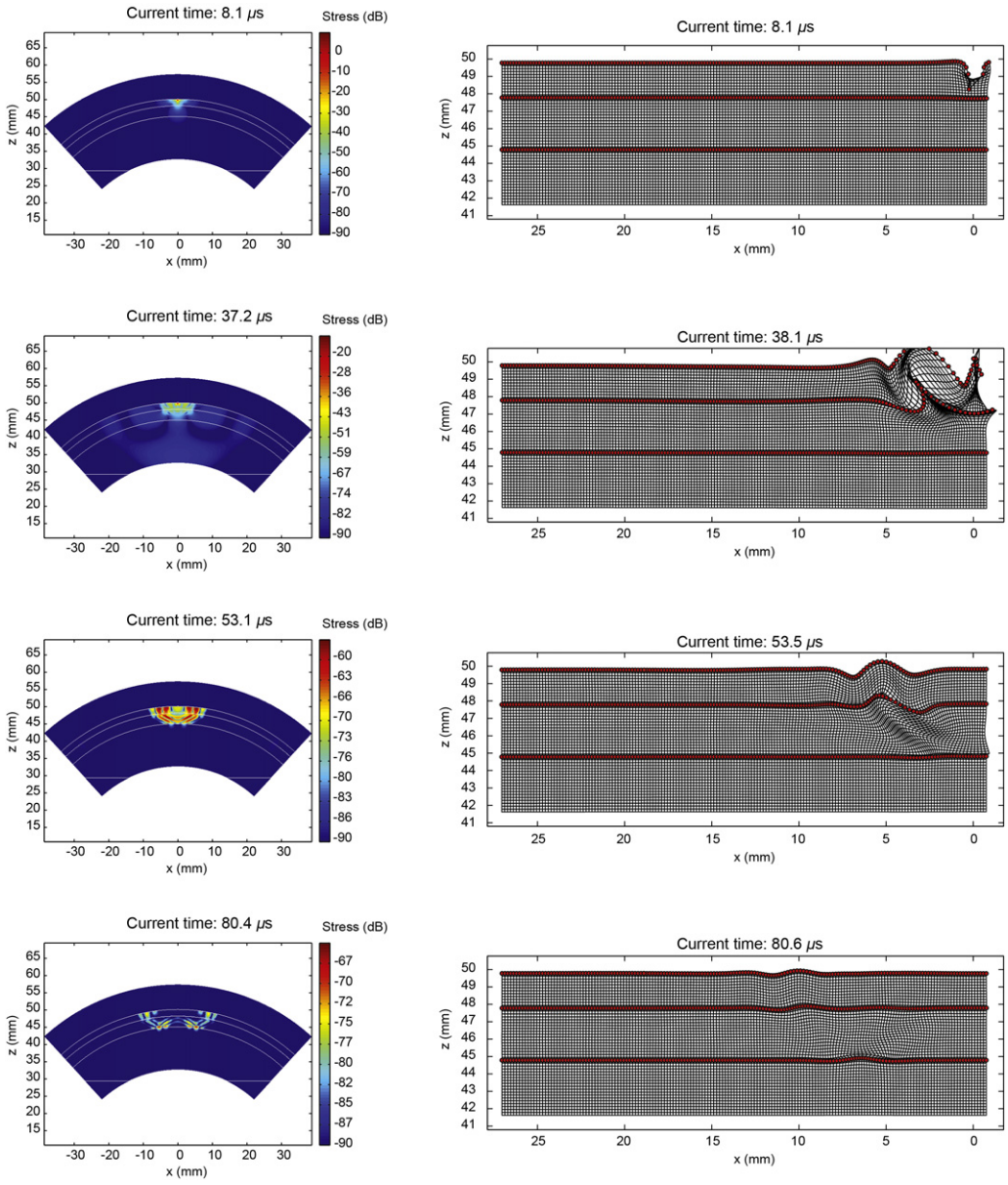


Fig. 4. Snapshots of the stress and the particle position for the fruit model with 1.8 dB/mm viscous loss.

4. Results

4.1. Experimental studies

These studies monitor the progress of the changes in the properties of the orange during storage under ambient conditions. Needless to say, dehydration increases with storage time (Fig. 2) due to weight loss through transpiration. Navelina dehydration reaches 3.8 kg/m^2 after 64 d under ambient conditions, while the Ortanique reaches 2.69 kg/m^2 in the same period under identical conditions. Fig. 2 can be explained as a non-linear relation with an asymptotic value. If we follow the hypothesis that the transfer rate of water from the orange to the atmosphere depends on the fruit surface area, the mass transfer coefficient and the difference between the water potential of the fruit and ambient conditions (De-Smedt et al., 2002), and we suppose the difference between fruit and ambient water potential is proportional to the water content of the fruit, then the next expression can be fitted to a good theoretical basis:

$$Dh(t) = a(1 - e^{-b \cdot t}) \quad (8)$$

where Dh is the dehydration during storage, kg/m^2, t the storage period, in days, and R the correlation coefficient.

Velocity of ultrasound through the orange peel increases with time (Fig. 3), from 120 to 220 m/s, approximately. Error bars, between 10 and 15%, are due to the intrinsic measurement procedure and the dispersion between the seven oranges. Here, differentiation between the two orange varieties is avoided. As in the case of dehydration, a non-linear asymptotic expression taking three parameters can relate velocity with time:

$$c(t) = c_0 + a(1 - e^{-b \cdot t}) \quad (9)$$

where c is the speed of ultrasound through the orange peel, m/s, and t is the storage period in days. The constant term is necessary

due to the fact that there is non-zero velocity on the day of the harvest.

The parameters obtained from the fit of experimental data to expressions (8) and (9) for Navelina and Ortanique can be seen in Table 3.

According to the accuracy of our experiment, the absorption of the ultrasonic waves in the orange peel remains constant during the 2 months of measurement. Navelina absorption remains at 1.8 ± 0.2 dB/mm and the Ortanique at 1.7 ± 0.3 dB/mm. The stability of absorption during storage time implies that this magnitude cannot be used as a quality control parameter, as has been demonstrated in Camarena et al., 2007. However, the absorption values measured here are very relevant for the discussion concerning the nature of the waves used to evaluate the elastic parameters of the orange peel.

4.2. Numerical studies

Fig. 4 on the left shows the snapshots of the normal stress modulus, illustrating the elastodynamic behavior of the modeled orange fruit with viscous loss. The figures show the three wave motions predicted: the most large wavelength pressure wave, the shear wave and the surface wave. In the sequence on the right, snapshots of the particle position are shown. From this, it can be appreciated how the longitudinal wave is strongly attenuated compared to the surface wave, which is the only one that can travel until 1 cm along the fruit's surface as it happens in the experiments.

Fig. 5 is a space-time plot. It reveals the recorded temporal signals versus the distance to the excitation source for several points on the surface of the simulated orange. Damping has not been considered in this simulation. From this plot, the propagation speed of the different waves existing in the simulation can be calculated by following the same procedure used in the experiment. The dotted white lines represent the fit for the traces of waves of equal phase in time and space. They show that two waves with different speeds can be detected on the surface of the orange model: the longitudinal wave (circles, 1576.0 m/s) and the surface wave (squares, 200.2 m/s).

A second model was simulated in order to take into account the high absorption of the vegetable fruit tissue, with the same parameters listed in Table 2 and setting the resistance coefficients to the attenuation values measured empirically (1.8 dB/mm, see Section 4.1). In this case, as can be seen from Fig. 6, only a low propagation speed wave is detected. The linear fit for the model with damping provides a wave speed value of 196.5 m/s, which concurs with the velocity measured in the experiment. From these simulations we can mainly conclude that our experimental device is sensitive only to the surface waves, i.e. due to the high damping in the orange peel, reflections of the longitudinal and shear waves in the inner parts of the orange can be overlooked.

A deeper analysis of the simulation results can allow us to determine what type of surface waves are being measured in the experiment. Fig. 7 shows the three components of the particle velocity of the wave as a function of depth (normalized to the longitudinal wavelength (λ_L)): the longitudinal component and the shear components, both vertical and horizontal. It can be seen that the particle velocity components are spatially offset, in such a way that the longitudinal component is at a maximum when the horizontal component is minimal. In addition, the wave is attenuated as a function of depth and the penetration length is approximately λ_L. Both are specific features of Rayleigh acoustic waves. Moreover, below a depth of about $0.2\,\lambda_L$ the velocity components are reversed, which means that the elliptical motion described by the particles also behaves in the same manner: on the surface the particle motion describes ellipses passing backwards in the sagittal plane, at a depth of $0.2\,\lambda_L$ the particle motion displays a minimum in all components

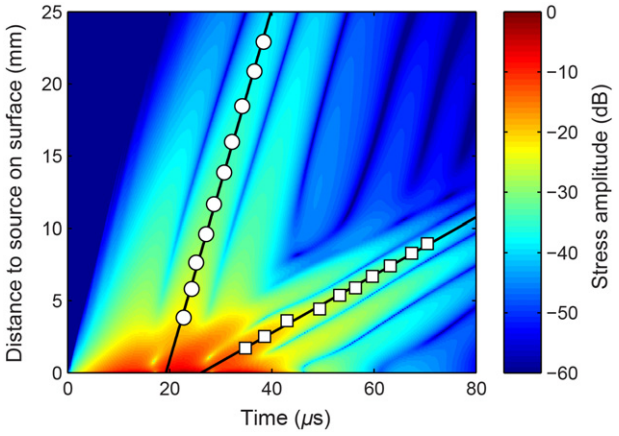


Fig. 5. Space-time diagram for the fruit model without damping. The circles represent the linear fit for longitudinal waves and the squares represent the fit for surface waves.

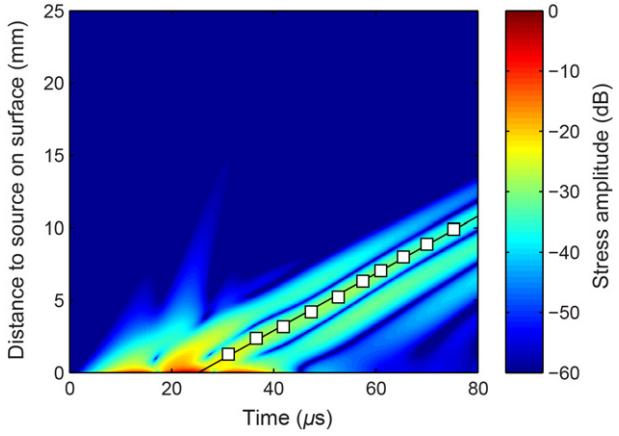


Fig. 6. Space-time diagram for the fruit model with 1.8 dB/mm viscous loss. The circles represent the linear fit for surface waves.

and below this depth, the elliptical motion of the particle turns in the opposite direction. From the results provided by the simulations, the physical analysis confirms that the waves propagating in the orange tissue are surface acoustic waves, more specifically Rayleigh waves.

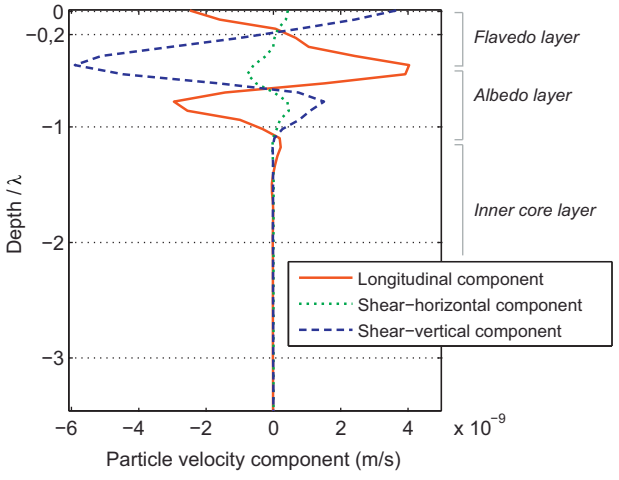


Fig. 7. Particle velocity amplitude components versus the orange peel depth normalized by the wavelength. On the right, the equivalent layer of the orange fruit.

4.3. Relation between the dehydration status and the elastic parameters

The main hypothesis considered to determine the elastic parameters of the orange peel is that the peel is a homogeneous water-like tissue, i.e. the longitudinal wave speed is similar to that in water ($c_P \approx 1500$ m/s) and Poisson's ratio falls in the range between 0.49 and 0.5 (Goss et al., 1978) which results in an established relation between the pure shear wave and the Rayleigh wave ($c_R \approx 0.95\, c_S$) (Malischewsky, 2005). From the linear elastic solid model, $c_S = (\mu/\rho)^{1/2}$ and $c_P = ((\lambda + 2\mu)/\rho)^{1/2}$, and the hypothesis listed above, the elastic parameters of the orange peel can be determined using the following expressions:

$$E = \rho \frac{((1/0.95)c_R)^2(-3{c_P}^2 + 4((1/0.95)c_R)^2)}{((1/0.95)c_R)^2 - {c_P}^2} \quad (10)$$

$$\nu = \frac{{c_P}^2 - 2((1/0.95)c_R)^2}{2{c_P}^2 - 2((1/0.95)c_R)^2} \quad (11)$$

where c_R is the ultrasonic measured speed, c_P is the longitudinal wave speed in water, ρ is the orange peel density, E is the Young modulus and ν is Poisson's ratio. Thus, using the proposed empirical model for the propagation speed shown in (8) and (9) and the previous relations (10) and (11), the evolution of the elastic parameters during storage time can be obtained for the two varieties of orange (Fig. 8). Moreover, the evolution of the Young modulus can be correlated with the measured dehydration process (Fig. 9); this figure reveals an almost linear relationship between the Young modulus and the measured dehydration of the orange peel.

5. Discussion

Most ultrasonic devices are used in quality evaluation of fruit and vegetables in an attempt to simply correlate the velocity and absorption of the ultrasonic wave traveling through the tissue with the quality parameter of interest. These being either sensory properties such as texture, physiochemical properties such as hydration degree, or mechanical properties, for example – firmness. Nevertheless, a solid knowledge about the type of wave that the ultrasonic device is measuring is necessary if we want to evaluate the elastic parameters of the medium, which are definitely of significance for its characterization.

The above simulation results show that the measured waves are surface Rayleigh waves, and therefore the elastic parameter can be calculated from the measured wave propagation speed values. Moreover, in this study has been found a relationship between the ultrasonically evaluated Young modulus and the measured dehydration of the orange peel, which means that the elastic parameters predicted by ultrasound are strongly related to an absolute physiological index. Therefore, the proposed ultrasonic test reported in this work is capable of determining the hydration state of the orange simply by measuring the propagation speed of the Rayleigh waves on the orange peel, and hence, can be used as a fruit quality index during postharvest processes.

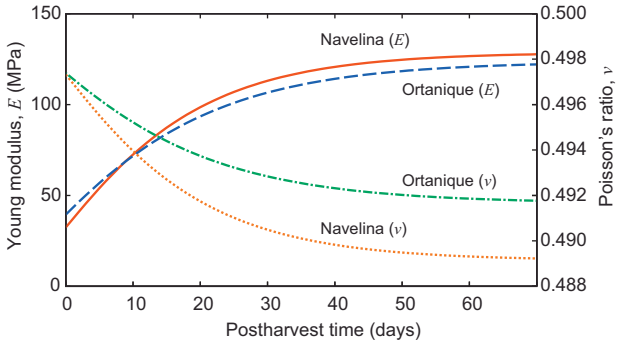


Fig. 8. Evolution of the predicted elastic parameters (Young's modulus and Poisson's ratio) during the storage time for the Navelina and Ortanique oranges.

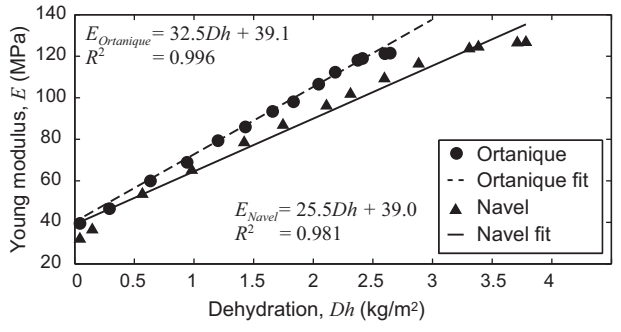


Fig. 9. Measured fruit dehydration versus the predicted Young's modulus for the Navelina and Ortanique oranges.

6. Conclusion

An experimental method has been used to evaluate the hydration state and the velocity of the ultrasonic waves in the peel of two varieties of oranges over their complete dehydration process. Both magnitudes change with storage time (hydration degree decreases and velocity increases) because the peel suffers many physiological changes during its dehydration process and ageing. So, the measurement of the ultrasonic wave velocity can be used to estimate the hydration degree of the orange. Otherwise, in order to evaluate the effect of the dehydration on the mechanical characteristics of the peel (Young modulus and Poisson's ratio) a better understanding is necessary on the nature of the ultrasonic waves that our experimental device is measuring. A solid elastic model has been proposed to simulate the wave propagation into the orange peel and a good agreement has been found between the ultrasonic wave velocity measured in the experiment and the velocity associated to a Rayleigh wave in the simulation. The values of the Young modulus obtained in the simulation fall in the range between 40 and 132 MPa, considerably higher than the values obtained from quasi-static measurements (1.57 MPa; Singh and Sreenivasula, 2006). The proposed model is able to explain the low values of velocity obtained in most of the experiments that make use of ultrasonic technology for fruit characterization (Camarena et al., 2007; Baryeh, 2000; Grotte et al., 2002; Jindal and Techasena, 1985; Bunyaphlanan, 1973): the ultrasonic waves detected are shear or Rayleigh waves, depending on the experimental configuration. Finally, this model allows the elastic parameters during the storage time of the fruit to be obtained from the values of the velocity measured and a linear relation has been found between the Young modulus and the dehydration degree of the orange peel. This relation can be used as a non-destructive method to estimate the hydration state of the orange.

Acknowledgements

This study was supported by the Programa de Apoyo a la Investigación y Desarrollo (PAID-05-09-002-618), (PAID-06-10-002-295) of Universidad Politécnica de Valencia. The authors would like to thank K. Y. Foo, from the University of Birmingham and P. Malischewsky from the University Friedrich-Schiller at Jena, for the fruitful discussions regarding surface acoustic waves.

References

Abbot, J.A., 1999. Quality measurement of fruits and vegetables. Postharvest Biol. Technol. 15 (3), 207–225.

Agusti, M., 2000. Citricultura. Mundi-Prensa, Madrid (in Spanish).

Auld, B.A., 1973. Acoustic Fields and Elastic Waves in Solids, vols. I and II. Wiley, New York.

Banab, K.K., Motazedian, D., 2010. On the efficiency of the multi-channel analysis of surface wave method for shallow and semi-deep loose soil layers. Int. J. Geophys. 2010, doi:10.1155/2010/403016, Article ID 403016.

Baryeh, E.A., 2000. Strength properties of avocado pear. J. Agric. Eng. Res. 76 (4), 389.

Bechar, A., Mizrach, A., Barreiro, P., Landahl, S., 2005. Determination of mealiness in apples using ultrasonic measurements. Biosyst. Eng. 91, 329–334.

Bossy, E., Talmant, M., Laugier, P., 2004. Three-dimensional simulations of ultrasonic axial transmission velocity measurement on cortical bone models. J. Acoust. Soc. Am. 115, 2314.

Bunyaphlanan, N., 1973. Mechanical proprieties of carrots tissues, Ph.D. thesis.

Butz, P., Homann, C., Tauscher, C., 2005. Recent developments in noninvasive techniques for fresh fruit and vegetable internal quality analysis. J. Food Sci. 70 (9), 131–141.

Camarena, F., Martinez-Mora, J.A., 2006. Potential of ultrasound to evaluate turgidity and hydration of the orange peel. J. Food Eng. 75, 503–507.

Camarena, F., Martínez-Mora, J.A., Ardid, M., 2007. Ultrasonic study of the complete dehydration process of orange peel. Postharvest Biol. Technol. 43, 115–120.

Chen, Y., Chew, W.C., 1998. A three-dimensional finite difference code for the modeling of sonic logging tools. J. Acoust. Soc. Am. 103, 702.

Chew, W.C., Liu, Q., 1996. Perfectly matched layers for elastodynamics: a new absorbing boundary condition. J. Comput. Acoust. 4, 341–359.

De-Smedt, V., Barreiro, P., Verlinden, B.E., Veraverbeke, E.A., De Baerdemaeker, J., 2002. A mathematical model for the development of mealiness in apples. Postharvest Biol. Technol. 25, 273–291.

Flitsanov, F., Mizrach, A., Liberzon, A., Akerman, M., Zauberman, G., 2000. Measurement of avocado softening at various temperatures using ultrasound. Postharvest Biol. Technol. 20, 279–286.

Gaete-Garreton, L., Vargas-Hernandez, Y., Leon-Vidal, C., Pettorino-Besnier, A., 2005. J. Food. Sci. 70, 187–191.

Goss, S.A., Johnston, R.L., Shnol, S.E., 1978. Comprehensive compilation of empirical ultrasonic properties of mammalian tissues. J. Acoust. Soc. Am. 64, 423–457.

Grotte, M., Duprat, F., Piétri, E., Loonis, D., 2002. Young's modulus, Poisson's ratio, and Lame's coefficients of golden delicious apple. Int. J. Food Prop. 5 (2), 333–349.

Hosokawa, A., 2008. Development of a numerical cancellous bone model for finite-difference time-domain simulations of ultrasound propagation. IEEE Trans. Ultrason. Ferroelectr. Freq. Control 55, 1219–1221.

Jindal, V.K., Techasena, O., 1985. Compression tests for measuring the firmness of potatoes. Trans. ASAE (Am. Soc. Agric. Eng.) 85–1072.

Krautkramer, J., Krautkramer, H., 1990. Ultrasonic Testing of Materials. Springer-Verlag, Heidelberg, Germany.

Malischewsky., P.G., 2005. Comparison of approximated solutions for the phase velocity of Rayleigh waves. Nanotechnology 16, 995–996.

Mizrach., C., 2000. Determination of avocado and mango fruit properties by ultrasonic technique. Ultrasonics 38, 717–733.

Mizrach, A., 2008. Ultrasonic technology for quality evaluation of fresh fruit and vegetables in pre-and postharvest processes. Postharvest Biol. Technol. 48, 315–330.

Mizrach, A., Galili, N., Rosenhouse, G., 2009. 3-D model of sound pressure field in a meridional section plane of fruit. Ultrasonics 49, 83–88.

Rayleigh, L., 1885. On waves propagated along the plane surface of an elastic solid. Proc. Lond. Math. Soc. 17, 4–11.

Schröder, C., Scott, W.R., 2002. On the stability of the FDTD algorithm for elastic media at a material interface. IEEE Trans. Geosci. Remote Sens. 40, 474–481.

Singh, K.K., Sreenivasula, B., 2006. Post-harvest physico-mechanical properties of orange peel and fruit. J. Food Eng. 73, 112–120.

Verlinden, J.A., De Smedt, V., Nicolaï, B.M., 2004. Evaluation of ultrasonic wave propagation to measure chilling injury in tomatoes. Postharvest Biol. Technol. 32, 109–113.